Mechanistic Aspects of the Reaction between Br_2 and Chalcogenone Donors (LE; E = S, Se): Competitive Formation of 10-E-3, T-Shaped 1:1 Molecular Adducts, Charge-Transfer Adducts, and $[(LE)_2]^{2+}$ Dications

M. Carla Aragoni,[a] Massimiliano Arca,[a] Francesco Demartin,[b] Francesco A. Devillanova,*[a] Alessandra Garau,[a] Francesco Isaia,[a] Francesco Lelj,[c] Vito Lippolis,*[a] and Gaetano Verani[a]

Abstract: The synthesis and spectroscopic characterisation of the products obtained by treatment of *N*,*N*′-dimethylimidazolidine-2-thione (**1**), *N*,*N*′-dimethylimidazolidine-2-selone (**2**), *N*,*N*′-dimethylbenzoimidazole-2-thione (**3**) and *N*,*N*′-dimethylbenzoimidazole-2-selone (**4**) with Br_2 in MeCN are reported, together with the crystal structures of the 10-E-3, T-shaped adducts **2**·Br_2 (**12**), **3**·Br_2 (**13**) and **4**·Br_2 (**14**). A conductometric and spectrophotometric investigation into the reaction between **1**–**4** and Br_2, carried out in MeCN, allows the equilibria involved in the formation of the isolated 10-E-3 (E = S, Se) hypervalent compounds to be hypothesised. In order to understand the reasons why S and Se donors can give different product types on treatment with Br_2 and I_2, DFT calculations have been carried out on **1**–**8**, **19** and **20**, and on their corresponding hypothetical $[LEX]^+$ cations (L = organic framework; E = S, Se; X = Br, I), which are considered to be key intermediates in the formation of the different products. The results obtained in terms of NBO charge distribution on $[LEX]^+$ species explain the different behaviour of **1**–**8**, **19** and **20** in their reactions with Br_2 and I_2 fairly well. X-ray diffraction studies show **12**–**14** to have a T-shaped (10-E-3; E = S, Se) hypervalent chalcogen nature. They contain an almost linear Br-E-Br (E = S, Se) system roughly perpendicular to the average plane of the organic molecules. In **12**, the Se atom of each adduct molecule has a short interaction with the Br(1) atom of an adjacent unit, such that the Se atom displays a roughly square planar coordination. The Se–Br distances are asymmetric [2.529(1) vs. 2.608(1) Å], the shorter distance being that with the Br(1) atom involved in the short intermolecular contact. In contrast, in the molecular adducts **13** and **14**, which lie on a two-fold crystallographic axis, the Br-E-Br system is symmetric and no short intermolecular interactions involving chalcogen and bromine atoms are observed. The adducts are arranged in parallel planes; this gives rise to a graphite-like stacking. The new crystalline modification of **10**, obtained from acetonitrile solution, confirms the importance of short intermolecular contacts in determining the asymmetry of Br-E-Br (E = S, Se) and I-Se-I groups in hypervalent 10-E-3 compounds. The analogies in the conductometric and spectrophotometric titrations of **1** and **2**–**4** with Br_2, together with the similarity of the vibrational spectra of **11**–**14**, also imply a T-shaped nature for **11**. The vibrational properties of the Br-E-Br (E = S, Se) systems resemble those of the Br_3^- and IBr_2^- anions: the Raman spectrum of a symmetric Br-E-Br group shows only one peak near 160 cm^{-1}, as found for symmetric Br_3^- and IBr_2^- anions, while asymmetric Br-E-Br groups also show an antisymmetric Br-E-Br mode at around 190 cm^{-1}, as observed for asymmetric Br_3^- and IBr_2^- ions. Therefore, simple IR and Raman measurements provide a useful tool for distinguishing between symmetric and asymmetric Br-E-Br groups, and hence allow predictions about the crystal packing of these hypervalent chalcogen compounds to be made when crystals of good quality are not available.

Keywords: density functional calculations · selenium · structure elucidation · sulfur · titrations · vibrational spectroscopy

Introduction

In recent years, the study of the donor–acceptor interaction between a variety of organic compounds LE containing atoms of Groups 15 and 16 (L = organic framework of the donor molecule, E = chalcogen atom) and halogens X_2 (X = I, Br) and interhalogens XY (X = I; Y = Br, Cl) has received great attention.[1–28] The growth of interest in this field of chemistry

[a] Prof. F. A. Devillanova, Prof. Dr. V. Lippolis, Dr. M. C. Aragoni, Dr. M. Arca, Dr. A. Garau, Dr. F. Isaia, Prof. G. Verani
Dipartimento di Chimica Inorganica ed Analitica
Università di Cagliari, S.S. 554, Bivio per Sestu
09042 Monserrato (CA) (Italy)
Fax: (+39) 070-6754456
E-mail: lippolis@unica.it

[b] Prof. F. Demartin
Dipartimento di Chimica Strutturale e Stereochimica Inorganica e Centro CNR
Università di Milano, Via G. Venezian 21
20133 Milano (Italy)

[c] Prof. F. Lelj
Dipartimento di Chimica, Via N. Sauro 85
85100 Potenza (Italy)

0947-6539/01/0714-3122 $ 17.50+.50/0

has been stimulated not only by the use of halogens and interhalogens to enhance the electric properties of S- or Se-based molecular conductors,[29] but also by an intrinsic interest in the different classes of compounds obtainable from reactions of the type LE + X_2 (or XY). In fact, together with charge-transfer (CT) adducts (10-X-2 hypervalent halogen compounds) bearing the linear E-X-X group,[2] donor oxidation products with chalcogen–halogen terminal bonds (LEX),[3f, 11b, 16a, 24] 10-E-3 hypervalent chalcogen compounds bearing the X-E-X linear group, two-coordinated halogens(I) with chalcogen ligands ($[LE\text{-}X\text{-}EL]^+$)[3b] and dications containing a chalcogen-chalcogen single bond ($[(LE)_2]^{2+}$)[4a, 11d] represent the most common types of product characterised crystallographically. In many cases, a very small change in the chemical environment of the donor atom or in the experimental conditions is enough to produce each of the above-mentioned products. New interest in this matter stems from the ability of halogen and interhalogen CT complexes to oxidise powdered metals in solvents of low polarity and under mild conditions to give complexes in which the metal exists in unusual oxidation states and coordination geometries.[30–32] Finally, interesting perspectives have also been found in the field of crystal engineering, since the different classes of halo-organo compounds can interact with halogens/halide anions, particularly I_2 and polyiodides, through soft–soft X···Y, E···X and E···Y interactions to give fascinating three-dimensional architectures.[3a, 4, 13b] This makes further exploration of reactions of the type LE + X_2 (or XY) very attractive in view of making predictions on the final products for each possible donor–acceptor couple. A first attempt in this direction was made by Husebye et al.,[12] although the chemical reaction diagram that they proposed needs to be supported by more experimental data. In the past, we have contributed to this type of chemistry mainly using thiones and selones as well as thioethers and selenoethers as donors and I_2 as acceptor. More recently, our studies have dealt with the use of the more acidic Br_2, IBr and ICl acceptors in reactions with the same sulfur and selenium donors. This paper reports on the synthesis and spectroscopic characterisation of the products obtained by treatment of **1**–**4** with Br_2, and the crystal structures of the T-shaped adducts **2**·Br_2 (**12**), **3**·Br_2 (**13**) and **4**·Br_2 (**14**). While several crystal structures of hypervalent T-shaped selenium compounds with Br_2 are reported in the literature,[2, 3e, 11a, 13b, 23–27] only one hypervalent T-shaped sulfur compound with Br_2 has yet been fully characterised by X-ray diffraction;[13a] hence **13** represents the second fully characterised, hypervalent, T-shaped sulfur compound.

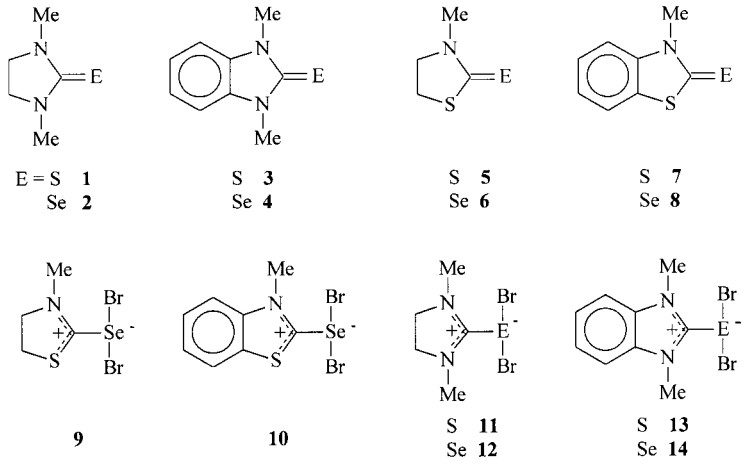

Results and Discussion

Solution studies: We have recently[5] reported the characterisation of the solid products obtained by treatment of *N*-methylthiazolidine-2(*3H*)-selone (**6**) and *N*-methylbenzothiazole-2(*3H*)-selone (**8**) with Br_2 (see Formula 1). Compound **8** always gives the corresponding 10-Se-3 hypervalent compound **10**, bearing the Br-Se-Br linear group, independently of the molar ratio between the reagents and the solvent (MeCN or CH_2Cl_2). In the same solvents, **6** gives the hypervalent compound **9** when a 1:1 molar ratio of Br_2 to **6** is used, and the ionic compound **15** when a 2:1 or higher reaction molar ratio is used. Interestingly, treatment of **8** with ICl in CH_2Cl_2 solution in a 1:1 molar ratio gives the CT adduct **8**·ICl,[3c] whereas compound **16**[10b] is obtained only if a 1:2 molar ratio of **8** to ICl is used. Analogous cations, such as **17** and **18**, have recently been obtained by treatment of *N*,*N*-dimethylselenourea[10a] and 4,5-bis(methylsulfanyl)-1,3-dithiole-2-thione,[13a] respectively, with Br_2. The cations **15**–**18** are formally derived from a carbon-chalcogen double-bond cleavage promoted by the halogen or the interhalogen.

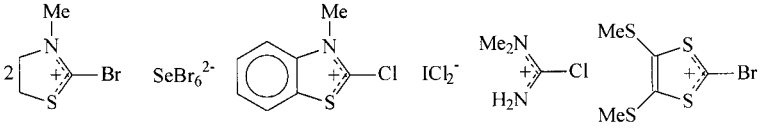

Conductometric and spectrophotometric titrations of **6** and **8** with Br_2 in MeCN proved very useful in identifying the various species in solution, and allowed us to hypothesise the equilibria reported in Scheme 1.[6] We therefore carried out analogous titrations on **1**–**4**. Figure 1a shows the results of conductometric titrations in MeCN between Br_2 and the sulfur donors **1** and **3**. As can be seen, the conductivity remains very low up to molar ratio of 1:1. Beyond this ratio it

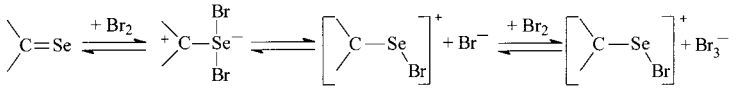

Scheme 1. Proposed equilibria involved in the reaction between Br_2 and compounds **6** and **8**.

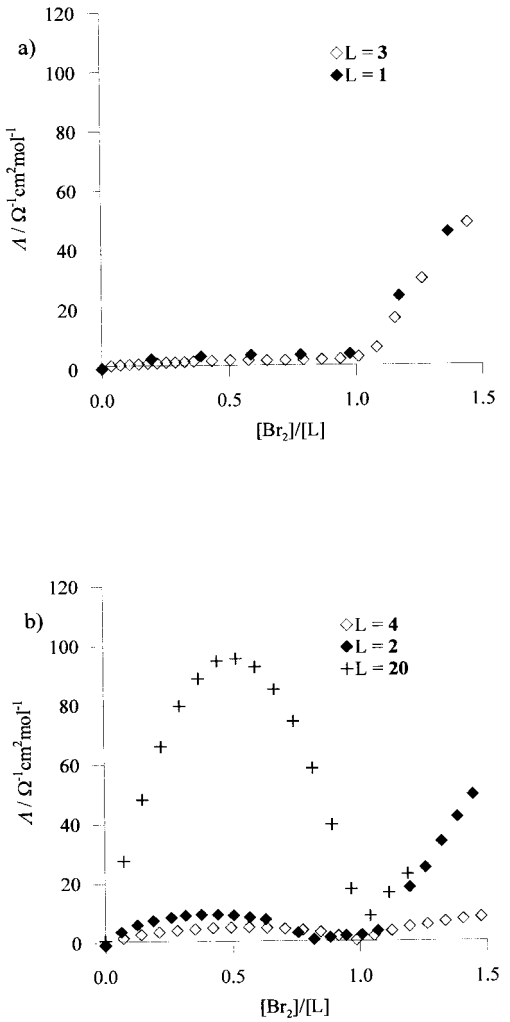

Figure 1. Conductometric titrations of a) S donors **1** and **3** and b) Se donors **2** and **4**. ([**1**], [**2**] = 1.8×10^{-2}, [**3**] = 8.4×10^{-3}, [**4**] = 2.7×10^{-3} M) with Br_2 (8.823×10^{-2} M) (MeCN; $T = 298$ K). In b), the conductometric titration of **20** ([**20**] = 2.16×10^{-3} M) has been included for comparison.

increases with addition of Br_2; this indicates that ionic species are being formed in solution. The stable, nonconducting compounds formed in the first part of the titration were isolated as solids on coincidence of the 1:1 molar ratio and, in the case of **3**, identified by X-ray diffraction analysis as the 10-S-3 hypervalent T-shaped adduct **3**·Br_2 (**13**) (see later). Unfortunately, no crystals suitable for X-ray crystal-structure determination were obtained for the adduct **1**·Br_2 (**11**), but the conductometric titration curve, similar to that found for **3**, and the vibrational properties of **11** (see below) also suggest a T-shaped nature for **11**.

Interestingly, the shape of the conductometric titration curves in Figure 1a resembles that found for the titration curve of **8**,[6] for which the equilibria reported in Scheme 1 were hypothesised. At present, this scheme should be considered a very simple model that accounts for the experimental data. However, the situation in the reaction medium could be much more complex. In particular, cation formation in the second step could be caused by different simultaneous processes, such as interaction of the hypervalent compound with a Br_2 molecule or interaction between two molecules of the hypervalent compound. Under these conditions, Scheme 1 should also be considered valid for the reactions of sulfur donors **1** and **3** with Br_2. In fact, the first equilibrium is proved to exist by the fact that spectra of solutions obtained by dissolving solid samples of **11** and **13** clearly show peaks related to the starting S donors **1** and **3** (see Table 1). Moreover, the extinction molar coefficients of the

Table 1. UV absorptions of **1**–**4** and their adducts **11**–**14** with Br_2 recorded in MeCN (logε in parentheses). Br_2 and Br_3^- bands are also included.

Compound	Absorption bands [nm]
1	219(4.64), 242(4.94)
1·Br_2 (**11**)[a]	218(4.50), 270(4.57)
2	234(4.21), 260(4.15)
2·Br_2 (**12**)[a]	206(4.24), 259(4.40)
3	230(4.46), 245(4.46), 311(4.70)
3·Br_2 (**13**)[a]	228(4.59), 277(4.51), 311(4.44)
4	230(4.32), 252(4.29), 322(4.62)
4·Br_2 (**14**)[a]	222(4.75), 266(4.61), 304(4.38)
Br_3^-	269(4.75)[b]
Br_2	268(2.16), 393(2.19)

[a] The positions of the bands of the hypervalent compounds **11**–**14** are taken from their spectra in MeCN solutions at concentrations of 4.4×10^{-5}, 7.13×10^{-5}, 4.73×10^{-5} and 2.473×10^{-5} M, respectively ($T = 298$ K). As discussed in the text, the spectra contain both the bands due to the hypervalent compounds and those due to the free **1**–**4**, in different amounts for the four compounds. The values for the molar extinction coefficients of the hypervalent compounds **11**–**14** must therefore be considered as only indicative, since they are involved in the equilibrium reactions shown in Scheme 1. Their solutions do not follow the Lambert–Beer law at different dilutions. [b] This value, measured on a freshly prepared solution of tetrabutylammonium tribromide (4.0×10^{-5} M), is very close to that (4.74) reported by A. I. Popov.[33]

bands typical of **11** and **13** change on varying the concentration, and the absorbance values do not obey the Lambert–Beer law for solutions at different dilutions. The formation of the Br_3^- anion, easily detected by UV-visible spectroscopy (see below), agrees well with the strong increase in conductivity beyond the 1:1 molar ratio (see Figure 1a). On the other hand, as in the case of **8**,[6] the very low but detectable conductivity values recorded in the first part of the titrations can be considered proof of the existence of the dissociation equilibrium of the T-shaped hypervalent compounds to give $[LSBr]^+$ and Br^- ionic species (according to Scheme 1). The hypothesis of the formation of $[LEBr]^+$ cations in solution is also supported by the fact that $[LEX]^+$ (E = S, Se; X = halogen) cations have in some cases been isolated in the solid state and characterised crystallographically.[3f, 11b, 16a]

The conductometric titration curves obtained for the selenium donors **2** and **4** are shown in Figure 1b. These curves show a different shape in the first part of the titration, resembling those found for conductometric titrations of **20**–**22** (the curve relating to **20** has been included in Figure 1b for comparison). For **20**, the conductivity values increase strongly on addition of Br_2, reaching a maximum for a Br_2/**20** molar ratio of 0.5:1.[7] On further addition of Br_2, conductivity starts to decrease and reaches a minimum at a Br_2/**20** molar ratio of 1:1.[7] The same behaviour is observed for **21** and **22**, with the

0947-6539/01/0714-3124 $ 17.50+.50/0 *Chem. Eur. J.* **2001**, *7*, No. 14

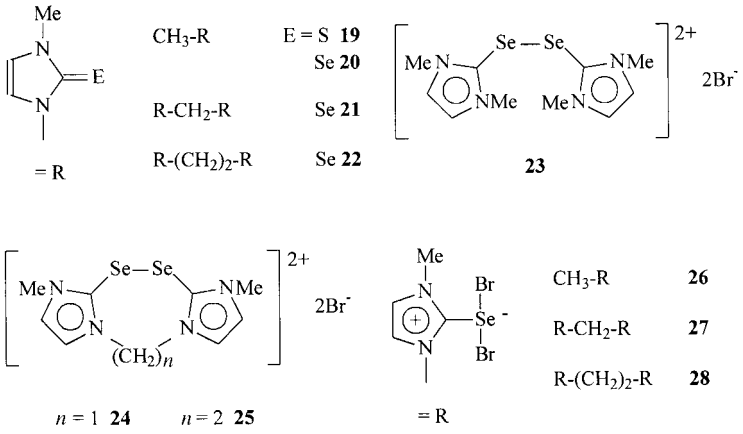

difference that the maximum conductivity value is reached for a 1:1 molar ratio, both these donors having two > C=Se groups in the molecule. For **20**–**22**, the isolated solid products corresponding to the maximum and minimum conductivity values proved to be the compounds **23**–**25** and **26**–**28**, respectively;[7] this indicates the almost quantitative formation of $[(LE)_2]^{2+}$ dication species featuring an Se–Se single bond in the first part of the titrations. In the second part, the dication species **23**–**25** are quantitatively transformed into the 10-Se-3 hypervalent compounds **26**–**28**.

Close inspection of the conductometric titration curves in Figure 1b shows that only compound **4** behaves like compound **20**, with much lower values for molar conductivity. Interestingly for compound **2**, the conductivity reaches its minimum value at a Br_2/**2** molar ratio of about 0.8:1 (the maximum having been reached at a molar ratio of about 0.4), and then begins to increase, first slowly and then very rapidly when the 1:1 molar ratio is reached. For either **2** or **4**, the maximum molar conductivity values remain below 15 $\Omega^{-1}\,cm^2\,mol^{-1}$, and the adducts **2**·$Br_2$ and **4**·Br_2 were isolated as crystals from the solutions corresponding to 1:1 molar ratios and identified by X-ray diffraction as the 10-Se-3 hypervalent T-shaped adducts **12** and **14** (see later). The behaviour of compounds **2** and **4** therefore seems to be intermediate between that of **20**–**22** and that of **1**, **3**, **6** and **8**: the shape of the titration curves in the first part can be explained by the simultaneous formation of $[(LE)_2]^{2+}$ dication species and 10-Se-3 hypervalent compounds. In both cases, however, the dications and the hypervalent compounds should be in equilibrium with the free donors **2** and **4**, since the spectra of solutions obtained by dissolving the solid samples of **12** and **14** clearly show the presence of peaks originating from free **2** and **4** (see Table 1), while the Lambert–Beer law is not obeyed on dilution.

The formation of the Br_3^- anion beyond the 1:1 molar reaction ratio, according to Scheme 1, was proved easily by spectrophotometric titrations in MeCN. The absorption bands of **1**–**4** and **11**–**14** recorded in MeCN solutions are listed in Table 1, together with those of Br_2 and Br_3^-. In all four spectrophotometric titrations (see Figure 2), the following common features can be observed: i) a general absorption

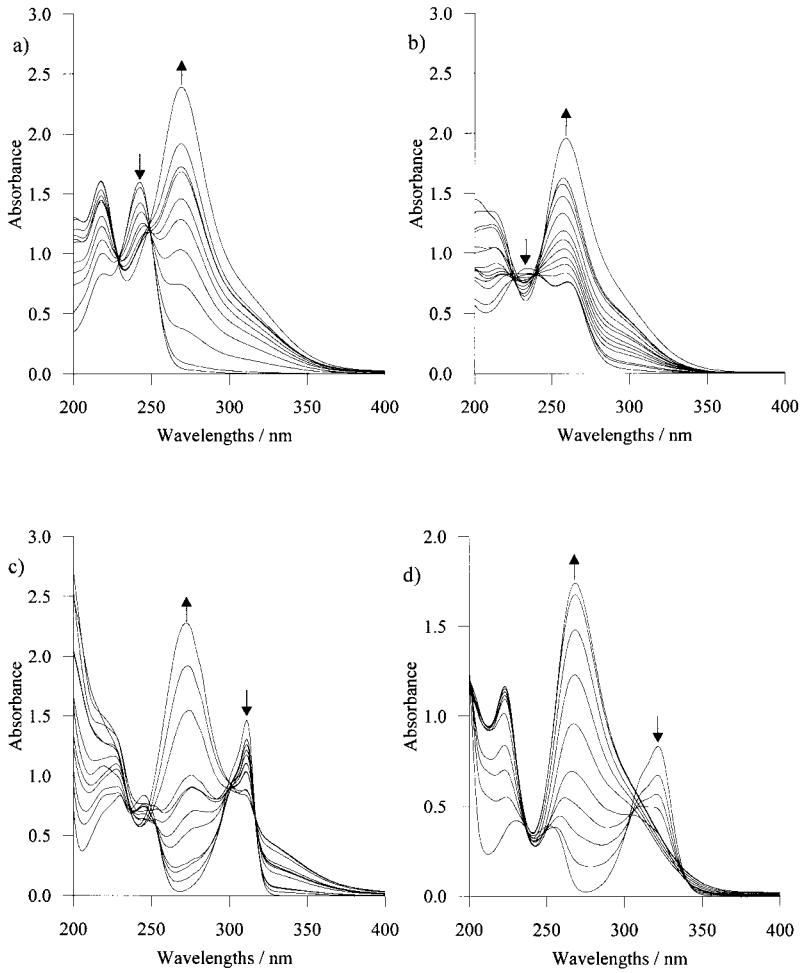

Figure 2. UV spectra of solutions with constant concentrations of the donors **1**–**4** with increasing quantities of Br_2 (T = 298 K; MeCN). a) [**1**] = 1.84×10^{-5} M; [Br_2]/[**1**] = 0, 0.6, 1.2, 1.8, 2.4, 3.0, 3.3, 3.6, 3.9, 4.5, 5.1. b) [**2**] = 5.4×10^{-5} M; [Br_2]/[**2**] = 0, 0.2, 0.3, 0.4, 0.42, 0.44, 0.5, 0.6, 0.7, 0.8, 0.9, 1.0, 1.2, 1.4. c) [**3**] = 2.92×10^{-5} M; [Br_2]/[**3**] = 0, 0.36, 0.55, 0.73, 0.92, 1.1, 1.46, 1.8, 2.2, 2.6, 2.9, 3.7. d) [**4**] = 2×10^{-5} M; [Br_2]/[**4**] = 0, 0.5, 0.75, 1.0, 1.25, 1.5, 1.75, 2.0, 2.25, 2.5.

decrease in the bands due to the free molecules **1**–**4** and a concurrent absorption increase in the bands due to the 10-E-3 adducts, ii) even if only those spectra of solutions with a Br_2/donor molar ratio up to 1:1 are considered, no isosbestic points are observed; this indicates the presence in solution—in low concentrations—of other species besides the free starting compounds and their 10-E-3 hypervalent adducts (E = Se, S) and iii) all the titrations are characterised by the appearance of a very strong absorption near 270 nm, due to the fact that either Br_3^- or the adducts **11**–**14** show a strong band near this value; however, this band increases more than the formation of **11**–**14** would lead us to expect. Its further increase when Br_2 is added beyond the complete formation of **11**–**14** clearly indicates an increasing amount of Br_3^-, (see Table 1) which is formed in solution according to Scheme 1. To this purpose, it should be pointed out that during the titrations of the sulfur donors **1** and **3**, the spectrophotometric curves take on the appearance of those of the corresponding hypervalent compounds only when the molar ratio is far above 1:1 (about 3:1 for **1** and 5:1 for **3**); this confirms that the formation of **11** and **13** is an equilibrium process. This seems to be in disagreement with the results of the conductometric titrations for the S donors, but it should be remembered that the two sets of titrations were carried out at very different concentrations: about 10^{-3} M in the conductometric titrations and 10^{-5} M in the spectrophotometric ones. On the other hand, only a small excess of Br_2 is enough to transform **2** and **4** almost completely into the corresponding Se-hypervalent compounds **12** and **14**. Thus, Scheme 1 also appears to account for the results of the spectrophotometric titrations of **1**–**4** with Br_2. In all four cases, the absence of isosbestic points in the spectrophotometric titrations corroborates the presence in solution of significant amounts of the various species as outlined in Scheme 1.

In order to understand the different chemical behaviour of **1**–**4**, **6**, **8** and **20**–**22** in the first part of the conductometric titrations, we carried out density functional theory (DFT) calculations[34–41] on compounds **1**–**8**, **19** and **20**, and also on the corresponding hypothetical $[LEX]^+$ cations (L represents the organic framework; E = S, Se and X = Br, I). Extension of the calculations to the $[LEI]^+$ species is useful in view of the large variety of solid products also obtained on treatment of these substrates with I_2. In fact, $[LEX]^+$ species were considered by Husebye[12] to play a key role as intermediates in the processes leading to the different types of products when LE organic donors were allowed to react with halogens. Furthermore, $[LEX]^+$ species can be regarded as deriving formally not only from the initially formed 10-E-3 hypervalent compound, but also from the 10-X-2 CT adduct by heterolytic breaking of an X–X bond. For the donors considered in this paper, calculations were aimed at predicting the products most likely to be formed if $[LEX]^+$ species are considered as key intermediates. Table 2 shows the NBO charges on the carbon, chalcogen and halogen atoms calculated at optimised geometries. On the basis of the charge distribution, the following observations can be made:

i) Comparison of the fractional charges on the chalcogen atoms in the hypothetical intermediate $[LEBr]^+$ species (in the range 0.191–0.281 e for S donors and 0.346–0.438 e for Se donors) and the charge on the terminal bromine (−0.074–0.048 e) clearly indicates that the attack of a nucleophile on the $[LEBr]^+$ cation is likely to occur on the chalcogen atom. If the nucleophile is Br^-, the corresponding chalcogen-hypervalent adduct is formed. Consequently, CT adducts between the donors under consideration and Br_2 are not to be expected. In fact, adducts featuring the Se-Br-Br linear group are unknown and only a very few cases have been reported for sulfur donors.[2]

ii) In contrast, the fractional charges on the chalcogen and iodine atoms in the $[LEI]^+$ cation show that the charge on the terminal iodine is always positive (from 0.131 to 0.183 e for the S donors and from 0.051 to 0.094 e for the Se donors), while that on the chalcogen is lower than that found in $[LEBr]^+$ (from 0.075 to 0.156 e for the S donors and from 0.233 to 0.314 e for the Se donors). Of the examined compounds, only **5** and **7** are likely to undergo attack of I^- on the sulfur atom in the corresponding $[LSI]^+$ cation to form hypervalent sulfur compounds that feature the I-S-I group, but this type of compound has never been isolated. In agreement with the experimental evidence so far collected, this seems to support the preferential formation of CT adducts from the reaction between sulfur donors and I_2. In contrast, for the examined selenium donors, the high positive charge on the selenium atom (from 0.346 to 0.438 e) compared with that on the terminal iodine (from 0.051 to 0.094 e) in $[LSeI]^+$ indicates a preferential tendency to form Se-hypervalent com-

Table 2. NBO charges Q [e] on C(2), E (E = S, Se), X (X = Br, I) atoms in LE (**1**–**8**, **19** and **20**) and in their corresponding $[LEX]^+$ ions. The last two columns give the differences ΔQ_E [e] between the Q_E in $[LEX]^+$ and LE.

L = E	E	Q_C L = E	Q_C $[LEBr]^+$	Q_C $[LEI]^+$	Q_E L = E	Q_E $[LEBr]^+$	Q_E $[LEI]^+$	Q_{Br} $[LEBr]^+$	Q_I $[LEI]^+$	ΔQ_E $[LEBr]^+$	ΔQ_E $[LEI]^+$
1	S	0.307	0.401	0.405	−0.256	0.196	0.075	0.046	0.179	0.452	0.331
2	Se	0.259	0.342	0.347	−0.228	0.356	0.233	−0.038	0.091	0.584	0.461
3	S	0.283	0.310	0.320	−0.229	0.191	0.083	0.001	0.131	0.420	0.312
4	Se	0.235	0.253	0.263	−0.208	0.346	0.236	−0.070	0.055	0.554	0.444
5	S	−0.080	−0.025	−0.020	−0.131	0.281	0.156	0.048	0.183	0.412	0.287
6	Se	−0.154	−0.095	−0.090	−0.100	0.438	0.314	−0.037	0.094	0.538	0.414
7	S	−0.103	−0.095	−0.086	−0.120	0.232	0.116	0.017	0.151	0.352	0.236
8	Se	−0.181	−0.163	−0.155	−0.088	0.396	0.280	−0.059	0.069	0.484	0.368
19	S	0.270	0.277	0.288	−0.283	0.196	0.085	0.004	0.135	0.479	0.368
20	Se	0.225	0.216	0.226	−0.268	0.355	0.244	−0.074	0.051	0.623	0.512

0947-6539/01/0714-3126 $ 17.50+.50/0 *Chem. Eur. J.* **2001**, *7*, No. 14

pounds rather than CT I_2 adducts; however, both types of adducts have been isolated.[2]

iii) The formation of $[(LE)_2]^{2+}$ dicationic species featuring a chalcogen–chalcogen single bond, obtained in the case of compounds **20**–**22** and hypothesised in solution as the conducting species in the cases of **2** and **4**, could be explained by a nucleophilic attack of the negatively charged chalcogen atom of a neutral LE molecule on the positively charged chalcogen atom of the $[LEBr]^+$ intermediate, with elimination of Br^-. From a qualitative point of view based on FMO theory,[42] the symmetries of the HOMOs of the donors, which in all the examined cases are *p* orbitals (out of molecular plane for **3**–**5**, **7**, **19** and **20**, and in the molecular plane for **1**, **2**, **6** and **8**), and the LUMOs of the $[LEBr]^+$ acceptors, which spread along the E–Br bond direction (see Figure 3 for **20** and [**20**–Br]$^+$), are appropriate for this nucleophilic attack, which should be

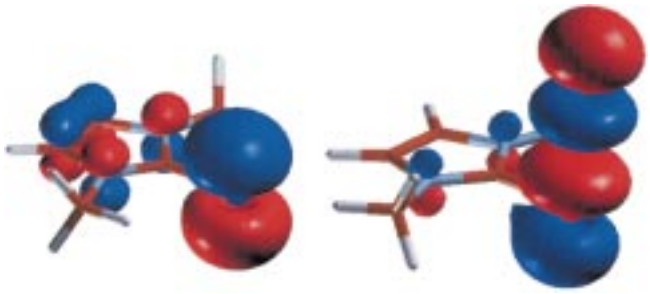

Figure 3. Representations of the HOMO of compound **20** (left) and the LUMO of the corresponding boromoselenide cation [**20**–Br]$^+$ (right).

favoured by a high value of the difference ΔQ_E (Table 2) between the charge on E in $[LEBr]^+$ and the charge on E in LE. As can be seen, the highest value of ΔQ_E (+0.623 e) is calculated for **20**, for which dication formation on treatment with Br_2 in MeCN solution is, as already mentioned, almost quantitative, and the salt **23** can be crystallised from solutions of molar ratios of 1:0.5 **20**/Br_2. For the compounds containing >C=S bonds given in Table 2, ΔQ_E is reduced to a value ranging from 0.352 to 0.479 e and no formation of $[(LS)_2]^{2+}$ dications has been experimentally observed for these donors, either in the solid state or in solution. Calculated values of ΔQ_E slightly higher than those found for the S donors are obtained for Se donors **6** and **8**, for which, once more, no dication formation has been observed. The ΔQ_E values calculated for **2** and **4** (0.584 and 0.554 e, respectively) are intermediate between the value calculated for **20**, and those calculated for **6** and **8**. Indeed, the conductometric titration curves in Figure 1b indicate the formation of significant quantities of dication species in the first part of the titration for **2** and **4** (see discussion above). On the basis of the ΔQ_E parameter, the tendency to form the $[(LE)_2]^{2+}$ dication species follows the decreasing order:

20 > **2** > **4** ≈ **6** > **8** ≈ **19** > **1** > **5** ≈ **3** > **7**.

In the last column of Table 2, the ΔQ_E values calculated in the case of $[LEI]^+$ cations are also reported. The decreasing order is the same as that found for $[LEBr]^+$. Accordingly, the direct reaction of **20** with IBr and ICl[3g] produced the same dication as for **23** but with different counteranions; whereas treatment of **2** with I_2 allowed the isolation of a mixed-valence compound in the solid state, in which an I_2 adduct unit is present together with a dication species $[\mathbf{2}_2]^{2+}$ with I_3^- as counter-ion.[3d]

As already mentioned, Husebye et al.[12] have very recently reported a chemical diagram collecting the different types of compounds that can be formed in reactions of the type LE + X_2 (L = organic framework; E = chalcogen atom; X = halogen) with the desirable aim of predicting the final products for each particular system of reagents. In that diagram, the formation of the dication $[(LE)_2]^{2+}$ was hypothesised as deriving from the attack of the LE donor on the chalcogen atom of the $[LEX]^+$ acceptor. These DFT calculations also support that hypothesis and also account for the fact that in some cases the dications can be formed in preference to the T-shaped hypervalent chalcogen compounds. In the diagram proposed by Husebye, however, the formation of the hypervalent compounds was explained by nucleophilic attack of an X_3^- ion on the E atom of the $[LEX]^+$ cation, with elimination of an X_2 molecule. Since, in reactions between Br_2 and compounds **1**–**4**, **6** and **8**, hypervalent chalcogen compounds are the only adducts formed before the 1:1 acceptor/donor molar ratio is exceeded, as shown by conductometric titrations, it is reasonable to propose that 10-E-3 hypervalent adducts might also be formed by the attack of an X^- ion on the chalcogen atom of the $[LEX]^+$ cation (reverse reaction of the second equilibrium in Scheme 1). At present, it is difficult to hypothesise all the possible pathways for transforming the $[(LE)_2]^{2+}$ dication into the corresponding hypervalent compounds on addition of Br_2, as observed for the donors **20**–**22**. One way to do this might be the reverse reaction of dication formation: breaking of the chalcogen-chalcogen bond promoted by X^- with formation of the $[LEX]^+$ cation and a molecule of LE, which undergoes an oxidative addition of Br_2 according to the first step in Scheme 1.

Solid state: On treatment of **1**–**4** with dibromine in MeCN, 1:1 adducts have been separated in the solid state. With the exception of **1**·Br_2 (**11**), the X-ray crystal structure determinations of these compounds show their 10-E-3 T-shaped hypervalent chalcogen adduct natures. Views of **12** and **13** are shown in Figures 4 and 5, respectively. Compound **14** is isostructural with **13** and the same labelling scheme as shown in Figure 5 has been adopted for it. Interatomic distances and angles for the three compounds are reported in Tables 3 and 4. The molecule of **12** contains an almost linear Br-Se-Br system [172.81(3)°], which is roughly perpendicular to the average plane of the molecule [Br(1)-Se-C(1)-N(1), torsion angle 93.6(6)°]. The arrangement of the molecules in the crystal is shown in Figure 6, in which a projection of the crystal packing along [010] is shown. The Se atom of each molecule is engaged in a short interaction with the Br(1) atom of an adjacent molecule [Se···Br(1) $(x, 1/2 - y, 1/2 + z)$]. 3.456(1) Å], so that the Se atom achieves a roughly square planar coordination. The Se–Br distances are asymmetric [2.529(1) vs. 2.608(1) Å], the shortest distance being that with the Br(1) atom involved in the short intermolecular contact.

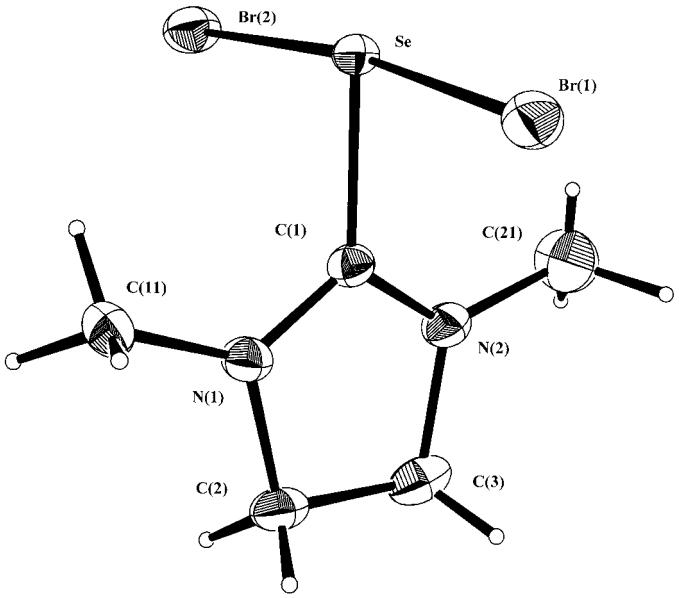

Figure 4. Molecular structure and atom labelling scheme of the T-shaped adduct **12** formed between *N*,*N*′-dimethylimidazoline-2-selone (**2**) and Br_2. The thermal displacement ellipsoids are given at the 30% probability level.

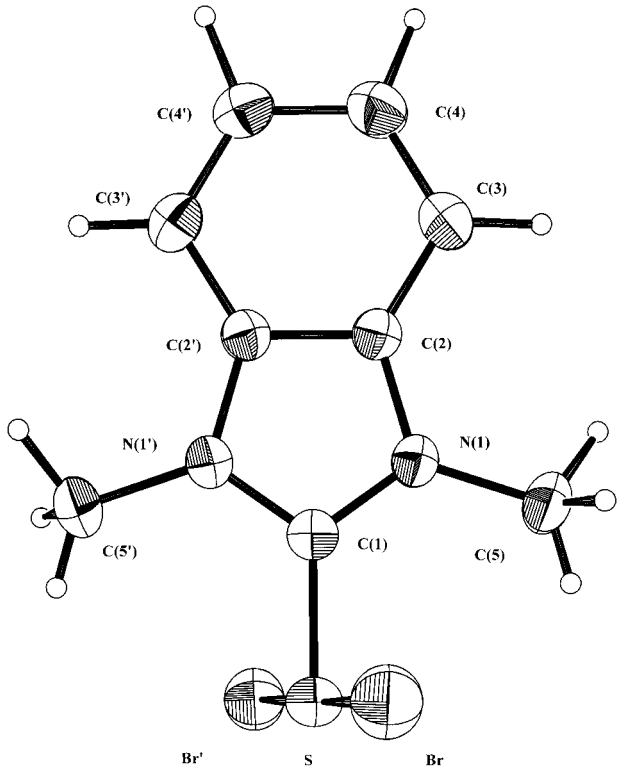

Figure 5. Molecular structure and atom labelling scheme of the T-shaped adduct **13** formed between *N*,*N*′-dimethylbenzimidazole-2-thione (**3**) and Br_2. The thermal displacement ellipsoids are given at the 30% probability level.

The molecular adducts **13** and **14** lie on a twofold crystallographic axis and therefore the Br-E-Br (E = S, Se) system, which is essentially linear, is symmetric. For them, no short interactions involving the chalcogen or bromine atoms of adjacent molecules are observed (Br···E > 4.1 Å) and the molecules are arranged in parallel planes; this gives rise to a graphite-like stacking. The Br-E-Br moiety is almost perpendicular to the remaining part of the molecule, which is planar: the dihedral angles Br-S-C(1)-N(1) and Br-Se-C(1)-N(1) are 76.0(1) and 72.2(2)°, respectively. The value of the Se–Br distance [2.572(1) Å] is exactly the average of the two asymmetric bonds found in **12**. Whilst in **13** and **14** the four C–N bond lengths in the five-membered ring are fairly similar, in **12** N(1)–C(1) is shorter than the other C–N bonds, which are otherwise similar to each other. The C–Se bond in **12** [1.931(6) Å] is very close in length to those found in **10**[5, 10a] and in the new modification of **10** [1.930(7) Å] (Table 5), whilst in **14** the C–Se bond is significantly shorter [1.889(1) Å]. In addition, the C–S bond in **13** [1.753(1) Å] is greatly lengthened with respect to the value found in **3** [1.671(8) Å].[43] On the whole, the carbon–chalcogen bonds can be considered as being very close to those corresponding to a single bond.

The crystal structures of **12**–**14** support the importance of the intermolecular contacts in generating asymmetry within the Br-E-Br (E = S, Se) group. In fact, in **12**, where a short

Table 3. Selected interatomic distances [Å] and angles [°] for $C_5H_{10}Br_2N_2Se$ (**12**)

Br(1)–Se	2.529(1)	N(1)–C(11)	1.440(10)
Br(2)–Se	2.608(1)	N(2)–C(1)	1.293(8)
Se–C(1)	1.931(6)	N(2)–C(3)	1.466(9)
N(1)–C(1)	1.306(8)	N(2)–C(21)	1.462(13)
N(1)–C(2)	1.459(8)	C(2)–C(3)	1.515(11)
Br(1)···Se	3.456(1)		
Br(1)-Se-Br(2)	172.81(3)	C(1)-N(2)-C(21)	128.8(7)
Br(1)-Se-C(1)	85.6(2)	C(3)-N(2)-C(21)	121.2(8)
Br(2)-Se-C(1)	87.4(2)	Se-C(1)-N(1)	124.2(5)
C(1)-N(1)-C(2)	111.3(6)	Se-C(1)-N(2)	122.8(5)
C(1)-N(1)-C(11)	127.6(6)	N(1)-C(1)-N(2)	113.0(6)
C(2)-N(1)-C(11)	121.0(6)	N(1)-C(2)-C(3)	101.8(6)
C(1)-N(2)-C(3)	109.8(6)	N(2)-C(3)-C(2)	103.9(6)

Table 4. Selected interatomic distances [Å] and angles [°] for $C_9H_{10}Br_2N_2E$.

	E = S (**13**)	E = Se (**14**)
Br–E	2.493(1)	2.572(1)
E–C(1)	1.753(1)	1.889(1)
N(1)–C(1)	1.337(2)	1.336(3)
N(1)–C(2)	1.386(3)	1.390(4)
N(1)–C(5)	1.465(3)	1.466(3)
C(2)–C(2′)	1.391(4)	1.393(5)
C(2)–C(3)	1.398(3)	1.388(4)
C(3)–C(4)	1.377(3)	1.364(4)
C(4)–C(4′)	1.418(5)	1.410(6)
Br···E	4.183(1)	4.139(1)
Br···Br	4.016(1)	4.077(1)
Br-E-Br′	179.38(4)	178.14(2)
Br-E-C(1)	89.69(2)	89.07(1)
C(1)-N(1)-C(2)	108.4(1)	108.8(2)
C(1)-N(1)-C5	126.6(2)	126.6(3)
C(2)-N(1)-C5	124.9(2)	124.6(2)
E-C(1)-N(1)	125.11(7)	125.3(2)
N(1)-C(1)-N(1′)	109.8(1)	109.5(3)
N(1)-C(2)-C(2′)	106.7(1)	106.5(1)
N(1)-C(2)-C(3)	131.2(2)	132.0(3)
C(2′)-C(2)-C(3)	122.1(1)	121.5(2)
C(2)-C(3)-C(4)	115.9(2)	116.7(3)
C(3)-C(4)-C(4′)	122.0(1)	121.7(2)

0947-6539/01/0714-3128 $ 17.50+.50/0 *Chem. Eur. J.* **2001**, *7*, No. 14

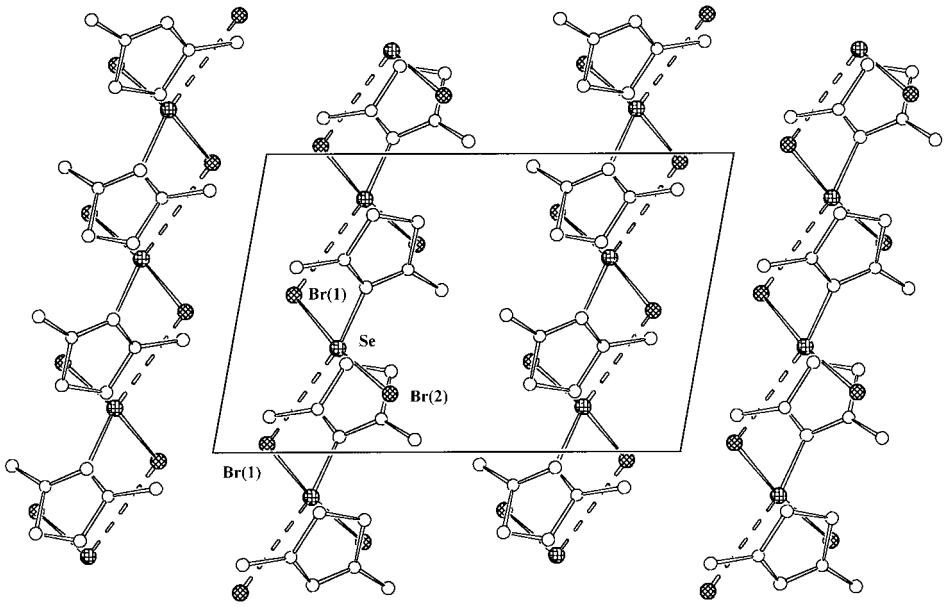

Figure 6. Crystal packing of compound **12**, showing the short Se···Br(1) intermolecular contacts.

Table 5. Selected interatomic distances [Å] and angles [°] for $C_8H_7Br_2NSSe$ (**10**).

Br(1)–Se	2.569(1)	N–C(8)	1.489(10)
Br(2)–Se	2.593(1)	S–C(1)	1.683(7)
Se–C(1)	1.930(7)	S–C(3)	1.753(7)
N–C(1)	1.325(8)	C(2)–C(3)	1.403(10)
N–C(2)	1.394(9)		
Br(1)···Se	3.354(1)		
Br(1)-Se-Br(2)	175.74(5)	C(1)-S-C(3)	91.8(4)
Br(1)-Se-C(1)	88.62(2)	S-C(3)-C(2)	108.4(6)
Br(2)-Se-C(1)	87.66(2)	Se-C(1)-N	125.3(6)
C(1)-N-C(2)	113.6(7)	Se-C(1)-S	121.2(4)
C(1)-N-C(8)	124.4(7)	S-C(1)-N	113.5(6)
C(2)-N-C(8)	122.0(6)	N-C(2)-C(3)	112.7(6)

Br(1)···Se contact of 3.456(1) Å is present, the Br-Se-Br moiety is asymmetric [Br(1)–Se 2.529(1) Å, Br(2)–Se 2.608(1) Å], while in **13** and **14** the shortest intermolecular contacts are 4.183(1) and 4.139(1) Å, respectively, and no asymmetry is found (Table 4). Also, the linearity of the Br-E-Br (E = S, Se) moiety is affected by these contacts, the angle being very close to 180° for **13** and **14** but only 172.81(3)° for **12**. A survey of the literature on Br-E-Br (E = S, Se) and I-Se-I systems shows that the situation observed in **12** is analogous to that found in $(C_6H_{11})_3PSeBr_2$,[10b] in 1,2-bis(3-methyl-4-imidazolin-2-ylium dibromoselenanide)-ethane,[7] and in the hypervalent selenium diiodine adducts with 1,3-dialkyl-4-imidazolin-2-selone (alkyl = Me,[3e] *i*Pr[11a]). In all these cases, only one of the two halogen atoms shows a contact with an adjacent adduct molecule, and the shortest halogen-chalcogen distance is that associated with the halogen atom involved in the short intermolecular contact, independently of the nature of the interacting atom. On the other hand, the structures of compound **10** (in the modification obtained from dichloromethane solutions[5, 10a]), of dibromo(tetramethylthiourea)selenium(II)[44] and of the adduct 1,2-bis(3-methyl-4-imidazolin-2-ylium diiodoselenanide)ethane,[3e] feature two short intermolecular contacts with formation of a four-membered, square-planar ring involving two selenium and two bromine atoms. The importance of the contacts in determining asymmetry in Br-E-Br (E = S, Se) moieties is further demonstrated by the new structural modification of **10** crystallised from acetonitrile solution (Table 5). In the structures of **10** reported earlier,[5, 10a] the presence of two dichloromethane molecules in the unit cell is crucial in determining the crystal packing. Compound **10**, when crystallised from MeCN solution, has only one Br atom engaged in interaction with the Se atom of an adjacent molecular adduct [3.354(1) Å]; this forms sinusoidal chains which propagate along the [001] direction (see Figure 7). Once again, the shortest Se–Br distance [Se–Br(1) 2.569(1); Se–Br(2) 2.593(1) Å] is that with the Br(1) atom involved in the short intermolecular contact.

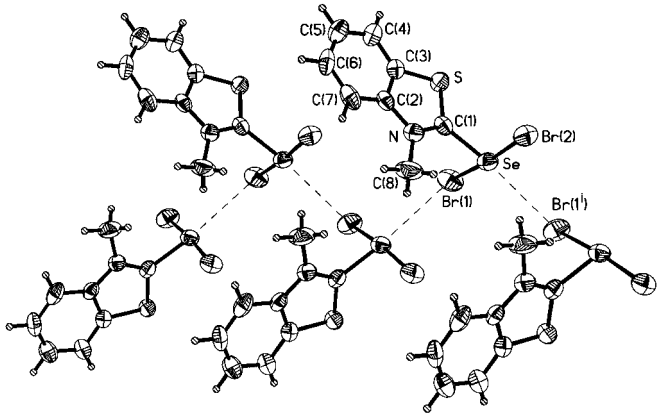

Figure 7. Crystal packing of the new crystalline modification of compound **10**, obtained from acetonitrile solution. The thermal displacement ellipsoids are given at a 50% probability level. Unlike in the previously reported structures for this compound, only one Se···Br(1) short intermolecular contact is present in this modification.

Different situations have been found in the bromine adducts of 1-thia-4-selenacyclohexane,[25] 4,5-bis(methylsulfanyl)-1,3-dithiole-2-thione,[13b] and selenocyanate anion,[23] in which both bromine atoms are involved in several short intermolecular contacts. The final result is either a practically symmetrical Br-Se-Br group [2.545(5) – 2.548(5) Å] in the adduct of 1-thia-4-selenacyclohexane,[25] or a quite asymmetric one [2.624(2) – 2.530(2) Å] in the $(SeCN)Br_2^-$ anion.[23] In the 4,5-bis(methylsulfanyl)-1,3-dithiole dibromine adduct reported by Bricklebank et al.,[13b] the asymmetry of the Br-S-Br group was attributed to the short intermolecular interactions, which also involved the sulfur atoms in the ring of the donor

molecule. For the four asymmetric structures containing the Br-Se-Br system reported by Akabori et al.,[26] it is not possible to verify the origin of the asymmetry, since the authors did not report the short intermolecular contacts. However, they did correlate the increasing asymmetry of the Se–Br bonds with the increasing total lengths of the Br-Se-Br group. Consequently, **13** and **14** represent the only known structures without intermolecular Br···E (E = S, Se) and Br···Br contacts; compound **13** in particular represents the first example reported in the literature of a 10-S-3 hypervalent sulfur adduct with two equal S–Br bonds. In contrast, the equality of the two Se–Br bonds found in the adduct of 2,3,7,8-tetramethoxyselenanthrene with Br_2 arises from the equivalence of the Se···Br intermolecular contacts involving both the bromine atoms.[27]

Compounds **11**–**14** have also been characterised by FT-IR and FT-Raman spectroscopy. Figure 8 shows the superimposed infrared and Raman spectra of **11**–**14** in the 300–50 cm^{-1} range. The Raman spectra of the four compounds

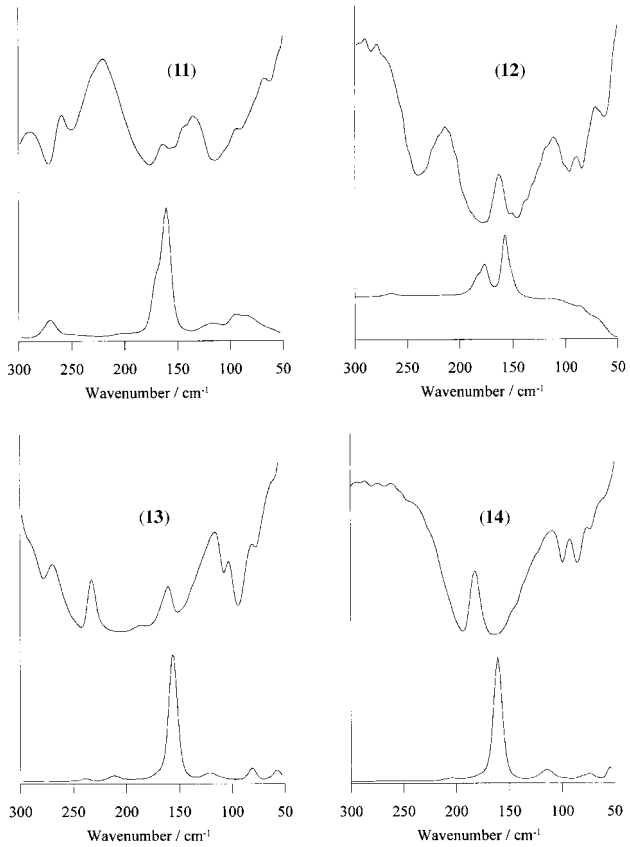

Figure 8. Superimposed FT-IR (top) and FT-Raman (bottom) spectra of compounds **11**–**14** in the low frequency region.

look very simple, since they are dominated by one or two peaks in the anticipated region of the frequencies of the Br-E-Br linear groups. In particular, **13** and **14**, the crystal structures of which suggest the presence of equal Br–E bond lengths, show only one peak, at 156 and 161 cm^{-1}, respectively (see spectra 3 and 4 in Figure 8), while **12**, which has an asymmetric Br-Se-Br group, shows two Raman peaks at 157 and 177 cm^{-1} (spectrum 2). The FT-IR spectra of these three compounds show one absorption close to the frequency of the most intense Raman peak and another broad absorption over 175 cm^{-1}; these can be attributed to the symmetric (ν_s) and antisymmetric (ν_{as}) stretching vibrations of Br-Se-Br, respectively.[45] It is important to note that the FT-Raman spectra of **26**–**28** look very similar to that of **12**, showing two peaks at 186 ± 6 and 152 ± 6 cm^{-1}, attributable to ν_{as} and ν_s of the Br-Se-Br three-body system, respectively. Accordingly, the crystal structures of **26**[15] and **28**[7] show asymmetries in the Br-E-Br bond lengths analogous to that found in **12**. The Raman spectrum of compound **11** (spectrum 1 in Figure 8) also looks similar to that of compound **12**, with the difference that the two peaks overlap—the one at the higher energy appearing as a shoulder. This also supports the T-shaped nature of **11**, probably with a slightly asymmetric Br-S-Br group. The vibrational properties of the Br-E-Br (E = S, Se) system resemble those of the $[Br\text{-}X\text{-}Br]^-$ (X = I, Br) anions. In fact, the Raman spectrum of a symmetrical Br-E-Br group in the presence of an inversion centre only shows one Raman peak near 160 cm^{-1}, as found in the symmetric Br_3^- and IBr_2^- anions, while asymmetric Br-E-Br groups display an additional antisymmetric Br-E-Br mode at around 190 cm^{-1}, as found in the asymmetric Br_3^- and IBr_2^- anions.[3f, 7, 46]

Conclusion

The reaction of LE (E = S, Se) chalcogen donor molecules with halogens and interhalogens can give different and unpredictable products. On the basis of all the types of products so far isolated and characterised, many authors have attempted to judge whether they could be formed from the same type of intermediate species . Husebye[12] hypothesised that this species was the $[LEX]^+$ (X = I, Br) cation derived from the initially formed 10-X-2 CT adduct or 10-E-3 hypervalent compound. The results described in this paper concerning the reactions between Br_2 and **1**–**4**, **6**, **8** or **20**–**22** that produce 10-E-3 hypervalent adducts or $[(LE)_2]^{2+}$ dications, clearly fit with the actual formation in solution of $[LEX]^+$ intermediate cations, at least for the restricted class of S donors and Se donors examined. In order to better understand both the role played by the $[LEX]^+$ cation and the reasons why the donors considered show different tendencies in forming $[(LE)_2]^{2+}$ dicationic species, 10-E-3 hypervalent adducts or 10-X-2 CT adducts when treated with I_2 or Br_2, we performed DFT calculations on the corresponding $[LEX]^+$ species. If we consider that $[(LE)_2]^{2+}$ dicationic species, 10-E-3 hypervalent adducts or 10-X-2 CT adducts can derive from a nucleophilic attack of the appropriate nucleophile on the $[LEX]^+$ cation from the chalcogen or halogen site, the calculated NBO charge distribution largely takes account of the experimental results. In fact, the charge distribution calculated for $[LSI]^+$ cations clearly indicates that for S donors the product most likely to be formed from the interaction of $[LSI]^+$ with X^- is the 10-I-2 CT adduct featuring the linear E-I-X group. In the case of Se donors, both 10-Se-3 hypervalent adducts with the I-Se-I group and 10-I-2 CT adducts could be formed, as confirmed experimentally. The formation of $[(LS)_2]^{2+}$ dication species from the attack of an

0947-6539/01/0714-3130 $ 17.50+.50/0 *Chem. Eur. J.* **2001**, *7*, No. 14

LS molecule on the sulfur atom of $[LSX]^+$ is very unlikely. On the other hand, the charge distribution calculated for $[LEBr]^+$ cations clearly indicates that 10-E-3 hypervalent compounds are very likely to occur as a consequence of the interaction of the $[LEBr]^+$ cation with Br^-. Indeed, Br_2 CT adducts with Se donors are unknown, and only a few cases have been reported for S donors. Considering the formation of $[(LE)_2]^{2+}$ dications as the result of a nucleophilic attack of an LE molecule on the chalcogen atom of $[LEBr]^+$ with elimination of Br^-, the parameter ΔQ_E (the difference between the charges on the chalcogen atom E in $[LEBr]^+$ and in LE) may be taken as a indication of the tendency of the considered donors to give dicationic species on treatment with Br_2. On the basis of this parameter, the following order—**20** > **2** > **4** ≈ **6** > **8** ≈ **19** > **1** > **5** ≈ **3** > **7**—can be given for the tendency of the considered donors to produce $[(LE)_2]^{2+}$ dications. This order largely agrees with the experimental observations. In conclusion, as also demonstrated by DFT calculations, the $[LEX]^+$ species plays a key role in the complex system of equilibria involved in the reactions of chalcogen donors with halogens and interhalogens. Extension of DFT calculations to a larger class of donors and to corresponding products obtainable on reaction with I_2, Br_2, IBr and ICl would be of great help in confirming this role and elucidating mechanistic aspects.

Experimental Section

Synthesis of 1–4: *N*,*N*′-dimethylimidazolidine-2-thione (**1**), *N*,*N*′-dimethylimidazolidine-2-selone (**2**), *N*,*N*′-dimethylbenzoimidazole-2-thione(**3**) and *N*,*N*′-dimethylbenzoimidazole-2-selone (**4**) were prepared according to the literature.[47]

Synthesis of 10–14: These compounds were prepared from MeCN solutions of the appropriate ligand and Br_2 in a 1:1 molar ratio. All the analytical data were consistent with the formulation of 1:1 molecular adducts **8**·Br_2 (**10**), **1**·Br_2 (**11**), **2**·Br_2 (**12**), **3**·Br_2 (**13**) and **4**·Br_2 (**14**), respectively.

Spectroscopic measurements: Spectrophotometric measurements were carried out in MeCN solutions by using a Varian model Cary 5 UV/Vis-NIR spectrophotometer equipped with a temperature controller accessory and connected to an IBM Personal System 2 Type 8513 TKQ S/N 55-DMR89. For **1–4**, spectra of several solutions with a constant donor concentration and increasing concentrations of Br_2 were recorded in the 200–400 nm range at a temperature of T = 298 K. The upper limit of the Br_2 concentration was chosen in order not to exceed an absorbance of 2.5 units at about 270 nm. The spectra of the hypervalent compounds **11–14** were recorded in MeCN solutions at concentrations of 4.4×10^{-5}, 7.13×10^{-5}, 4.73×10^{-5} and 2.473×10^{-5} M, respectively, (T = 298 K). The shapes of the spectra in solution change on changing the concentration, and the solutions at different dilutions do not follow the Lambert–Beer law.

Conductivity measurements: Conductometric titrations were carried out at $T = 298$ K in MeCN solution in a standard thermostatted cell with a Model 120 microprocessor conductivity meter analytical control. The k cell (1.23 cm^{-1}) was determined by measuring the conductivity of three solutions of KCl (previously kiln-dried for 12 hours) in doubly distilled water of 0.1, 0.01 and 0.001 M at $T = 298$ K. Conductivity was recorded 5 minutes after each Br_2 addition in order to allow the temperature to stabilise. The Br_2 concentration in MeCN was measured with a standard aqueous $Na_2S_2O_3$ solution (0.100 M) according to traditional methods.

DFT calculations: Quantum chemical calculations were carried out by using the commercially available Gaussian 94 suite of programs.[34] Density functional calculations[35] were performed by using the hybrid Becke 3LYP functional (which uses a mixture[36]of Hartree–Fock and DFT exchange along with DFT correlation: the Lee–Yang–Parr correlation functional together with Becke's gradient correction).[37] For all calculations, Schafer, Horn and Ahlrichs' pVDZ[38] basis sets were used for C, H, N, O, S and Se, while LANL2DZ basis sets together with effective core potentials (ECP)[39] were adopted for halogen atoms. Numerical integration was performed by using the FineGrid option, which indicated that a total of 7500 points were used for each atom. In order to achieve SCF convergence for compounds **1**

Table 6. Crystallographic data.

Compound	**10**	**12**	**13**	**14**
formula	$C_8H_7Br_2NSSe$	$C_5H_{10}Br_2N_2Se$	$C_9H_{10}Br_2N_2S$	$C_9H_{10}Br_2N_2Se$
mass [amu]	387.99	336.93	338.08	384.97
space group	$P2_1/c$ (n.14)	$P2_1/c$ (n.14)	$C2/c$ (n.15)	$C2/c$ (n.15)
a [Å]	8.296(2)	12.768(9)	13.101(4)	13.260(3)
b [Å]	19.139(6)	9.925(5)	9.777(2)	9.947(2)
c [Å]	7.788(3)	8.211(9)	9.411(2)	9.178(2)
β [°]	115.23(3)	100.34(6)	109.58(1)	108.52(1)
V [Å^3]	1118.6(6)	1024(1)	1135.7(5)	1147.9(4)
Z	4	4	4	4
$F(000)$	728	632	656	728
ρ_{calcd} [g cm^{-3}]	2.304	2.186	1.977	2.227
$\mu(Mo_{K\alpha})$ [cm^{-1}]	106.4	113.1	72.1	101.0
T [K]	293(2)			
radiation	graphite monochromatised $Mo_{K\alpha}$ [0.71073 Å]			
diffractometer	Enraf-Nonius CAD4			
scan mode	ω	ω	ω	ω
scan speed [° min^{-1}]	0.5–2	2–3	0.5–2	0.5–2
scan width [°]	$1.4 + 0.350\tan\theta$	$1.1 + 0.350\tan\theta$	$1.0 + 0.35\tan\theta$	$1.0 + 0.35\tan\theta$
θ range [°]	3–27	3–26	3–27	3–27
independent reflections	2425	1993	1240	1335
observed reflections [$I > 3\sigma(I)$]	1012	1171	982	952
transmission factors	0.73–1.00	0.50–0.97	0.71–1.53	0.50–1.00
parameters refined	118	105	65	66
final R and Rw indices[a]	0.029, 0.031	0.041, 0.047	0.029, 0.041	0.033, 0.042
largest diff. peak	0.47(11)	0.96(14)	0.45(9)	0.91(13)
hole [e Å^{-3}]	−0.48(11)	−0.60(14)	−0.60(9)	−0.78(13)

[a] $R = [\Sigma(F_o - k|F_c|)/\Sigma F_o]$, $Rw = [\Sigma w(F_o - k|F_c|)^2/\Sigma w F_o^2]^{1/2}$.

and **19**, the V shift option was employed, thus shifting Kohn–Sham orbital energies by 100 mHartrees. Moreover, the maximum number of SCF cycles was raised from the default value (64) to 512 and 768 for **19** and **20**, respectively. After geometry optimisation, NBO[40] calculations were performed for each molecule by using the converged density matrix corresponding to the equilibrium geometries. The Kohn–Sham orbital drawings reported in Figure 3 were elaborated with Molden 3.6.[41] Calculations were performed on an IBM Risc 6000 550 H, DECServer 4000 and a VAIER Intel Pentium III 450 MHz personal computer running Linux Suse 6.3.

X-Ray crystal structure determination: Details of the data collection and refinement of the structures are reported in Table 6. Crystals were mounted on a glass fibre in a random orientation. Preliminary examination and data collection were performed with graphite monochromatised $Mo_{K\alpha}$ radiation (0.71073 Å) on an Enraf–Nonius CAD4 computer-controlled kappa axis diffractometer. Cell constants and an orientation matrix for data collection were obtained from least-squares refinement by using the setting angles of 25 reflections. The data were collected at room temperature by using a variable scan rate (2 to 20° min^{-1} in omega). Three representative reflections were measured every hour to check the stability of the crystals under X-ray exposure: these measurements revealed no decay of the scattering power of the crystal. Lorentz and polarisation corrections, together with an empirical absorption correction performed as described in [48], were applied to the data. The structures were solved by using direct methods (MULTAN) and difference Fourier syntheses, and refined in full-matrix, least-squares, the function minimised being $\Sigma w(|F_o|-|F_c|)^2$. All the hydrogen atoms were seen in a difference Fourier map and introduced into the structure model. Scattering factors were taken from Cromer and Waber.[49] Anomalous dispersion effects were included in F_c; the values for $\delta f'$ and $\delta f''$ were those of Cromer.[50] All calculations were performed on an 80486/33 computer with Personal SDP software.[51] Atomic coordinates, displacement parameters, bond lengths and angles for **12**, **13**, **14** and the new modification of **10** have been deposited at the Cambridge Crystallographic Data Centre as supplementary publications no. CCDC-155182 to CCDC-155185. Copies of the data can be obtained free of charge on application to CCDC, 12 Union Road, Cambridge, CB2 1EZ, UK (fax: (+44) 1223-336033; e-mail: deposit@ccdc.cam.ac.uk

Acknowledgements

The project was carried out as part of the "Progetto Finalizzato Materiali Speciali per Tecnologie Avanzate II" of the "Consiglio Nazionale delle Ricerche".

[1] M. C. Aragoni, M. Arca, F. Demartin, F. A. Devillanova, A. Garau, F. Isaia, V. Lippolis, G. Verani, *Coord. Chem. Rev.* **1999**, *184*, 271.
[2] M. C. Aragoni, M. Arca, F. Demartin, F. A. Devillanova, A. Garau, F. Isaia, V. Lippolis, G. Verani, *Trends Inorg. Chem.* **1999**, *6*, 1, and references therein.
[3] a) M. Arca, F. Demartin, F. A. Devillanova, A. Garau, F. Isaia, V. Lippolis, G. Verani, *J. Chem. Soc. Dalton Trans.* **1999**, 3069; b) F. Demartin, F. A. Devillanova, F. Isaia, V. Lippolis, G. Verani, *Inorg. Chem.* **1993**, *32*, 3694; c) F. Demartin, F. A. Devillanova, A. Garau, F. Isaia, V. Lippolis, G. Verani, *Polyhedron*, **1999**, *18*, 3107; d) F. Demartin, F. A. Devillanova, F. Isaia, V. Lippolis, G. Verani, *Inorg. Chim. Acta* **1997**, *255*, 203; e) F. Bigoli, M. A. Pellinghelli, P. Deplano, F. A. Devillanova, V. Lippolis, M. L. Mercuri, E. F. Trogu, *Gazz. Chim. It.* **1994**, *124*, 445; f) F. Cristiani, F. A. Devillanova, F. Demartin, F. Isaia, V. Lippolis, G. Verani, *Inorg. Chem.* **1994**, *33*, 6315; g) F. Bigoli, F. Demartin, P. Deplano, F. A. Devillanova, F. Isaia, V. Lippolis, M. L. Mercuri, M. A. Pellinghelli, E. F. Trogu, *Inorg. Chem.* **1996**, *35*, 3194.
[4] a) A. J. Blake, F. A. Devillanova, R. O. Gould, V. Lippolis, S. Parsons, C. Radek, M. Schröder, *Chem. Soc. Rev.* **1998**, *27*, 195.
[5] F. A. Devillanova, P. Deplano, F. Isaia, V. Lippolis, M. L. Mercuri, S. Piludu, G. Verani, F. Demartin, *Polyhedron* **1998**, *17*, 305.
[6] M. Arca, F. Demartin, F. A. Devillanova, A. Garau, F. Isaia, V. Lippolis, S. Piludu, G. Verani, *Polyhedron* **1998**, *17*, 3111.
[7] F. Bigoli, P. Deplano, F. A. Devillanova, V. Lippolis, M. L. Mercuri, M. A. Pellinghelli, E. F. Trogu, *Eur. J. Inorg. Chem.* **1998**, 137, and references therein.
[8] A. J. Blake, F. A. Devillanova, A. Garau, F. Isaia, V. Lippolis, S. Parsons, M. Schröder, *J. Chem. Soc. Dalton Trans.* **1999**, 525, and references therein.
[9] a) F. Bigoli, P. Deplano, P. Ienco, C. Mealli, M. L. Mercuri, M. A. Pellinghelli, G. Pintus, G. Saba, E. F. Trogu, *Inorg. Chem.* **1999**, *38*, 4626; b) P. Deplano, J. R. Ferraro, M. L. Mercuri, E. F. Trogu, *Coord. Chem. Rev.* **1999**, *188*, 71, and references therein.
[10] a) P. D. Boyle, W. I. Cross, S. M. Godfrey, C. A. McAuliffe, R. G. Pritchard, S. J. Teat, *J. Chem. Soc. Dalton Trans.* **1999**, 2845; b) S. M. Godfrey, S. L. Jackson, C. A. McAuliffe, R. G. Pritchard, *J. Chem. Soc. Dalton Trans.* **1998**, 4201; c) P. D. Boyle, J. Christie, T. Dyer, S. M. Godfrey, I. R. Howson, C. McArthur, B. Omar, R. G. Pritchard, G. Rh. Williams, *J. Chem. Soc. Dalton Trans.* **2000**, 3106, and references therein.
[11] a) N. Kuhn, T. Kratz, G. Henkel, *Chem. Ber.* **1994**, *127*, 849; b) N. Kuhn, H. Bohnen, G. Henkel, *Z. Naturforsch.* **1994**, *49b*, 1473; c) N. Kuhn, H. Kotowski, T. Kratz, G. Henkel, *Phosphorus Sulfur Silicon*, **1998**, *136*, 517.
[12] M. D. Rudd, S. V. Linderman, S. Husebye, *Acta Chem. Scand.* **1997**, *51*, 689, and related papers.
[13] a) N. Bricklebank, P. J. Skabara, D. E. Hibbs, M. B. Hursthouse, K. M. Abdul Malik, *J. Chem. Soc. Dalton Trans.* **1999**, 3007; b) P. S. Skabara, N. Bricklebank, R. Berridge, S. Long, M. E. Light, S. J. Coles, M. Hursthouse, *J. Chem. Soc. Dalton Trans.* **2000**, 3235.
[14] a) A. J. Arduengo, E. M. Burgess, *J. Am. Chem. Soc.* **1977**, *99*, 2376; b) A. J. Arduengo, H. V. Rasila Dias, J. C. Calabrese, *Chem. Lett.* **1997**, 143; c) A. J. Arduengo, F. Davidson, H. V. Rasila Dias, J. R. Goerlich, D. Khasnis, W. J. Marshall, T. K. Prakasha, *J. Am. Chem. Soc.* **1977**, *119*, 12742.
[15] a) D. J. Williams, D. VanDerveer, B. R. Crouse, R. R. Raye, T. Carter, K. S. Hagen, M. Brewer, *Main Group Chem.* **1997**, *2*, 61; b) D. J. Williams, K. D. Wynne, *Inorg. Chem.* **1976**, *15*, 1449.
[16] a) E. Seppälä, F. Ruthe, J. Jeske, W.-W. du Mont, P. G. Jones, *Chem. Commun.* **1999**, 1471; b) W.-W. du Mont, *Main Group Chem. News* **1994**, *2*, 18; c) J. Jeske, W.-W. du Mont, P. G. Jones, *Chem. Eur. J.* **1999**, *5*, 385; d) S. Kubiniok, W.-W. du Mont, S. Pohl, W. Saak, *Angew. Chem.* **1988**, *100*, 434; *Angew. Chem. Int. Ed. Engl.* **1988**, *27*, 431; e) W.-W. du Mont, F. Ruthe, *Coord. Chem. Rev.* **1999**, *189*, 101; f) V. Stenzel, J. Jeske, W.-W. du Mont, P. G. Jones, *Inorg. Chem.* **1997**, *36*, 443.
[17] E. Krawczyk, A. Skowronska, *Phosphorus Sulfur Silicon* **1990**, *51*, 329.
[18] W. A. S. Nandana, J. Passmore, P. S. White, *J. Chem. Soc. Dalton Trans.* **1983**, 526.
[19] P. K. Baker, S. D. Harris, M. C. Durrant, D. L. Hughess, R. L. Richards, *Acta Crystallogr. Sect. C* **1995**, *51*, 697.
[20] M. M. A. Hamed, M. B. Mohamed, M. R. Mahmoud, *Bull. Chem. Soc. Jpn.* **1994**, *67*, 2006.
[21] F. Freeman, J. W. Ziller, H. N. Po, M. C. Keindl, *J. Am. Chem. Soc.* **1988**, *110*, 2586.
[22] F. H. Herbstein, W. Schwotzer, *J. Am. Chem. Soc.* **1984**, *106*, 2367.
[23] S. Hauge, K. Marøy, *Acta Chem. Scand.* **1992**, *46*, 1166.
[24] U. Geiser, H. H. Wang, J. A. Schlueter, J. M. Williams, J. L. Smart, A. C. Cooper, S. K. Kumar, M. Caleca, J. D. Dudek, K. D. Carlson, J. Ren, M.-H. Whangbo, J. E. Schirber, W. R. Bayless, *Inorg. Chem.* **1994**, *33*, 5101.
[25] L. Battelle, C. Knobler, J. D. McCullough, *Inorg. Chem.* **1967**, *6*, 958.
[26] M. Miura, Y. Takanohashi, Y. Habata, S. Akabori, *J. Chem. Soc. Perkin Trans. 1* **1995**, 1719, and related papers.
[27] P. Berges, W. Hinrichs, G. Klar, *J. Chem. Research (S)* **1986**, 362.
[28] A. W. Cordes, S. L. Craig, M. S. Condren, R. T. Oakley, R. W. Reed, *Acta Crystallogr. Sect. C* **1986**, *42*, 922.
[29] J. R. Ferraro, J. M. Williams, *Introduction to Synthetic Electrical Conductors*, Academic Press, New York, **1987**.
[30] a) F. Bigoli, P. Deplano, F. A. Devillanova, V. Lippolis, M. L. Mercuri, M. A. Pellinghelli, E. F. Trogu, *Inorg. Chim. Acta* **1998**, *267*, 115; b) M. Arca, F. A. Devillanova, A. Garau, F. Isaia, V. Lippolis, G. Verani, G. L. Abbati, A. Cornia, *Z. Anorg. Allg. Chem.* **1999**, *625*, 517.

  0947-6539/01/0714-3132 $ 17.50+.50/0

[31] S. M. Godfrey, C. A. McAuliffe, R. G. Pritchard, J. Sheffield, *Inorg. Chim. Acta* **1999**, *292*, 213, and related papers.
[32] F. Bigoli, P. Deplano, M. L. Mercuri, M. A. Pellinghelli, G. Pintus, A. Serpe, E. F. Trogu, *Chem. Commun.* **1998**, 2351.
[33] A. I. Popov, R. F. Swensen, *J. Am. Chem. Soc.* **1955**, *77*, 3724.
[34] Gaussian 94 (Revision D.1 and E.1), M. J. Frisch, G. W. Trucks, H. B. Schlegel, P. M. W. Gill, B. G. Johnson, M. A. Robb, J. R. Cheeseman, T. A. Keith, G. A. Petersson, J. A. Montgomery, K. Raghavachari, M. A. Al-Laham, V. G. Zakrzewski, J. V. Ortiz, J. B. Foresman, C. Y. Peng, P. Y. Ayala, M. W. Wong, J. L. Andres, E. S. Replogle, R. Gomperts, R. L. Martin, D. J. Fox, J. S. Binkley, D. J. Defrees, J. Baker, J. P. Stewart, M. Head-Gordon, C. Gonzalez, J. A. Pople, Gaussian, Inc., Pittsburgh PA, **1995**.
[35] a) J. Labanowsky, J. Andzelm. *Density Functional Methods in Chemistry.* Springer, New York, **1991**; b) E. S. Kryachko, E. V. Ludeña. *Energy Density Function Theory of Many Electron Systems*, Kluver Academic, NL. **1990**.
[36] A. D. Becke, *J. Chem. Phys.* **1993**, *98*, 1372.
[37] C. Lee, W. Yang, R. G. Parr, *Phys. Rev. B* **1988**, **37**, 785.
[38] A. Schafer, H. Horn, R. Ahlrichs, *J. Chem. Phys.* **1992**, *97*, 2571.
[39] a) P. J. Hay, W. R. Wadt, *J. Chem. Phys.* **1985**, *82*, 299; b) J. V. Ortiz, P. J. Hay, R. L. Martin, *J. Am. Chem. Soc.* **1992**, *114*, 2736.
[40] A. E. Reed, L. A. Curtiss, F. Weinholt. *Chem. Rev.* **1988**, *88*, 899.
[41] G. Schaftenaar, J. H. Noordik, *J. Comput.-Aided Mol. Design* **2000**, *14*, 123.
[42] I. Fleming in *Frontier Orbitals and Organic Chemical Reactions*, Wiley, New York, **1976**.
[43] G. R. Form, E. S. Raper, T. C. Downie, *Acta Crystallogr. Sect. B* **1976**, *32*, 345.
[44] K. J. Wynne, P. S. Pearson, M. G. Newton, J. Golen, *Inorg. Chem.* **1972**, *11*, 1192.
[45] These attributions are consistent with those reported for tetramethylselenourea dibromine adduct: M. Bodelsen, G. Borch, P. Klaeboe, P. H. Nielsen, *Acta Chem. Scand. Ser. A* **1980**, *34*, 125.
[46] a) G. C. Hayward, P. J. Hendra, *Spectrochim. Acta Part A* **1967**, *23*, 2509, and references therein; b) A. G. Maki, R. Forneris, *Spectrochim. Acta Part A* **1967**, *23*, 867.
[47] a) F. A. Devillanova, G. Verani, *Ren. Sem. Fac. Sc. Univ. Cagliari*, **1977**, *47*, 255; b) F. Cristiani, F. A. Devillanova, A. Diaz, G. Verani, *J. Chem. Soc. Perkin Trans. 2* **1984**, 1383.
[48] F. Demartin, C. M. Gramaccioli, T. Pilati, *Acta Crystallogr. Sect. C* **1992**, *48*, 1.
[49] D. T. Cromer, J. T. Waber, *International Tables for X-Ray Crystallography*, *Vol. IV*, Kynoch, Birmingham, England, **1974**, Table 2.2B.
[50] D. T. Cromer, *International Tables for X-Ray Crystallography*, *Vol. IV*, Kynoch, Birmingham, England, **1974**, Table 2.3.1.
[51] a) B. Frenz, *Comput. Phys.* **1988**, *2*, 42; b) B. Frenz, *Crystallographic Computing 5*, Oxford University Press, **1991**, Chapter 11, pp. 126 – 135.

Received: December 28, 2000 [F2975]